Cell, Volume *139*

Supplemental Data
The IFITM Proteins Mediate Cellular Resistance to Influenza A H1N1 Virus, West Nile Virus, and Dengue Virus

Abraham L. Brass, I-Chueh Huang, Yair Benita, Sinu P. John, Manoj N. Krishnan, Eric M. Feeley, Bethany Ryan, Jessica L. Weyer, Louise van der Weyden, Erol Fikrig, David J. Adams, Ramnik J. Xavier, Michael Farzan, and Stephen J. Elledge

SUPPLEMENTAL DISCUSSION

To provide a more integrated view of influenza A virus-host interactions, we compared the functional genomic results of our study with the fly-based genetic screen, and the literature mining data of the Reactome project (http://www.reactome.org, Fig. S2). Reactome is an expertly-curated resource of human biologic pathways, including the host-viral interactions occurring during influenza A virus infection. The resulting protein network extension analysis provided functional support for the role of six host factors in the Reactome influenza A virus infection pathway ($p=0.027$), and revealed first-order (direct) interactions between 37 host factors found in this screen and those listed in the Reactome ($p=0.007$, Dataset S2). To identify potential key intermediates, human and fly host factors detected in the RNAi screens were used to select proteins that are significantly ($p<0.05$, Fig. S2) connected given the number of their known interactors. Fourteen proteins were predicted as potentially important in the flu lifecycle, including the RNA helicase DHX15, the nuclear transporter TNPO2 and the mRNA surveillance and export protein UPF3A (Fig. S2). Such testable hypotheses of possible host-viral "nodes and edges" will likely continue to emerge as comprehensive screening efforts and meta-analyses are completed.

The Drosophila-based screen demonstrated that influenza A virus can function across phylogenetic kingdoms, from post-entry to transcription of vmRNAs . Such versatility in a non-arbovirus, may arise from flu's need to rely on highly conserved protein-interaction surfaces and pathways when infecting diverse species (man, birds and swine). It follows then that host directed antiviral therapies (HDAVs) against influenza viruses may be more readily transferable across species as well. While the similarities in these two screen data sets underscore the utility of the Drosophila platform, that strategy none-the-less required the use of a pseudotyped entry mechanism and recombinant viral reporter genes, somewhat limiting the extent of the viral lifecycle surveyed (Hao et al., 2008). We also posit it less likely that restriction factors, like IFITM3, would be present in pathogen-naïve model system organisms or cell lines, which have not been under selective pressure to generate viral-specific defenses.

Careful analysis also found that splicing of the viral proteins NEP (NS2) and M2 did not occur in the fly cells, which would preclude evaluation of host proteins that interact with these factors, or the portions of the viral lifecycle they support (Hao et al., 2008). With this in mind, it is interesting that our screen uniquely enriched for RNA processing and splicing factors (Fig. 2, Dataset S1A, S2). However, decreased expression of NEP or M2 would not be predicted to alter the early viral lifecycle processes or the surface expression of HA (Lamb and Krug, 2001). Thus, flu's reliance on splicing may represent a previously unappreciated role for M2 or NEP, or more likely an indirect effect created by limiting the processing of one or more host factors.

Both essential and non-essential splicing components were found to play a role in infection. For example, we found Trimethylguanosine synthase 1 (TGS1) which generates 2,2,7-trimethylguanosine (TMG) caps on snRNAs, many of which are essential for splicing (Mouaikel et al., 2002) and TGS1 and TMG caps are both non-essential for either yeast or human cell

growth (Lemm et al., 2006). A synthetic lethality screen using *tgs1Δ* yeast recovered multiple RNA splicing factors, including U2 snRNP components (Hausmann et al., 2008). Importantly, that study showed that human TGS1 functionally complements yeast Tgs1(Hausmann et al., 2008). The author's concluded that splice sight recognition by TMG cap-containing snRNPs was functionally redundant with the intrinsic splice site binding affinity of the identified genetic modifiers (Hausmann et al., 2008).

As noted in the main text, our screen detected TGS1 along with a large number of splicing factors, including U2 snRNP proteins. Therefore, upon comparing our data with the yeast synthetic lethal screen's results, we hypothesize that TGS1's role in modifying snRNAs underlies flu's dependence on this enzyme, and that flu is more sensitive than its host to perturbations in splice site recognition and/or splicing efficiency. Such instances illustrate that mammalian RNAi screens can effectively combine with classic model system genetics in the hunt for viral susceptibilities.

While most antiviral drugs target viral proteins, the discovery of genetic dependencies on host proteins establishes the possibility that drugs to host proteins could provide a strong antiviral response if they are not toxic to the host. In addition to TSG1, several other host factors have enzymatic activities (Dataset S1F) that could allow them to be easily screened for inhibitors. Influenza A virus' need to rely on highly conserved protein-interaction surfaces and pathways when infecting diverse species (man, birds and swine), also suggests that HDAVs against influenza viruses may be more readily transferable across species as well. Such inhibitors, alone or in combination, could effectively treat acute influenza A viral infections and could be preventative during an epidemic.

SUPPLEMENTAL EXPERIMENTAL PROCEDURES:

siRNA screen: To identify host factors required for influenza A virus infection, a high-throughput RNAi-based screen was undertaken on an arrayed library targeting 17,877 genes (Dharmacon siARRAY siRNA Library (Human Genome, G-005000-05, Thermo Fisher Scientific, Lafayette, CO, the remaining 3,244 pools of the original 21,121 gene library were not screened because the vast majority have been retired due to revised refseq annotation or other concerning characteristics). siRNAs were transiently reverse transfected into the U2OS cells at a 50 nM final concentration, using a final concentration of 0.32% Oligofectamine (Invitrogen, Carlsbad, CA) in a 384-well format (384 well, black plastic, clear bottomed assay plate, Corning 3712). The next day, 5 uL of fresh complete media (DMEM with 10% FBS, Invitrogen) was added to the outer two wells at the plate margins to decrease edge effects. After 72 h of siRNA-mediated gene knockdown, the medium was removed and the cells were infected with the Influenza A/Puerto Rico/8/34 (PR8, ATCC VR-1469), at an moi of approximately 0.2-0.3 in 40 uL complete media. After 12 h, the media was removed and the cells were then fixed with 4% formalin and stained with purified anti-HA monoclonal antibody (Hybridoma HA36-4-5.2, Wistar Institute), followed by an Alexa Fluor 488 goat anti-mouse secondary at 1:1,000 (A11001, Invitrogen). The cells were imaged on an automated Image Express Micro (IXM) microscope (Molecular Devices), and images were analyzed using the Metamorph Cell Scoring software program (Molecular Devices Inc.). A negative control (NT, siCONTROL Non-Targeting siRNA #2, Dharmacon D-001210-02), and positive control siRNA against NXF1 (SMARTpool M-013680-01) and NP (Dharmacon custom siRNA siGenome synthesis, see below) were present on each plate. Wells containing either buffer alone, or an siRNA pool directed against Polo like kinase one (PLK1, Dharmacon) were present on all plates transfected. The screen was performed in triplicate.

In the primary screen, siRNA pools were classified as hits (decreased infection) if the average of the triplicate plates showed that the percentage of core positive cells was less than 55% of the

plate mean. In addition, siRNA pools were classified as toxic to the host cell and eliminated from further evaluation, if the final cell number was less than 40% of the mean of the plate. Pools which increased infection by greater than 200% of the plate mean were also selected as hits (increased infection).

The validation round screen in which the four individual oligos comprising each pool were placed into separate wells, and screened again using identical methods as above. siRNA pools were considered validated if two or more of the individual oligos scored (55% or less infected cells (decreased infection)) or 150% or greater infected cells (increased infection) as compared to the negative control wells on the plate, in either both part one and two or part two alone, and the cell number was not less than 40% of the average of the negative control wells on the plate. In the noted instances (Dataset S1A, farthest right column), transfections were done with a final concentration of 20 nM siRNA to minimize host cell toxicity while still creating a virustatic hypomorphic state. The percent of infected cells relative to controls, as well as the normalized cell numbers for each of the individual genes that confirmed with two or more siRNAs is provided in Dataset S1. Visual spot inspections of control images were done thoughout the screen to confirm the accuracy of the automated imaging and cell scoring systems.

Cell lines and culture conditions: U2OS, A549, MDCK, Vero E6, primary Chicken embryonic fibroblast (ChEFs), Huh 7.5.1 and HeLa cells were grown in DMEM (Invitrogen Cat#11965) with 10% FBS (Invitrogen). WI-38 cells were cultured in DMEM (Invitrogen Cat#10569), containing 1X MEM non-essential amino acids (Invitrogen Cat#11140, 10 mM stock/100X) and 15% FBS. HeLa-CD4 (HeLa-T4+) cells were generously provided by the NARRRP, and kindly contributed by Dr. Richard Axel.

Mouse embryonic fibroblasts: Adult *IfitmDel*$^{+/-}$ mice (Lange et al., 2008) were intercrossed and fibroblasts (MEFs) derived from embryos at day 13.5 of gestation, as described previously (Nagy et al., 2003). MEFs were genotyped by PCR (Thermo-Start *Taq* DNA Polymerase, ABgene; Epsom, UK) on embryo tail genomic DNA using primers to detect the presence of the wildtype allele (F: 5'-aac atg cct tgc atc cct gga gtt cct tct aaa gga-3'; R: 5'-ccc taa aac act tag cag tga ccc ctc aca agc c-3'; 450 bp band) and the targeted/knockout allele (F: 5'-act cta gcc aga gtc ttg cat ttc tca gtc cta aac-3'; R: 5'-tct agt aca gtc ggt aag aac aaa ata gtg tct atc a-3'; 650 bp band). The PCR cycle profile was as follows: 1 cycle at 95°C for 15 min followed by 35 cycles at 95°C for 30 s, 62°C for 1 min, and 72°C for 45 s, with a final cycle of 72°C for 5 min. All studies were performed on MEFs isolated from three independent matings. MEFs were cultured in DMEM, containing 10% FBS, 1X MEM essential amino acids, 1X 2-Mercapto-ethanol (Gibco).

Cytokines: Human interferon γ (Invitrogen Cat #PHC4031) was used at 100-300 ng/ml, human interferon α A (Invitrogen Cat# PHC4014) was used at 500-2500 U/ml. Cells were incubated with cytokines for 24 h prior to viral infection. Murine interferon α (PBL Interferon Source, Cat # 12100-1) and IFN-γ (PBL Interferon Source, Cat # 12500-2) were used at 500-2500 U/ml., and 100-300 ng/ml respectively.

Transfections: For follow-up experiments with U2OS and HeLa cells, we plated 2200 cells per well in clear bottom 96 well plates (Corning 3603), one day prior to transfections. Cells were transfected with siRNAs at 50 nM final concentration and Oligofectamine at 0.4% in DMEM containing 15% FBS. For WI-38 primary fibroblast cells, 6000 cells were plated per well one day prior to transfection in Corning 3603 plates. The following day, transfections were done using Lipofectamine 2000 and 100 nM final concentration siRNA. siRNA-mediated target gene depletion occurred over three days, then cells were challenged with one of the following: influenza A virus (H1N1) A/PR/8/34, influenza A (H1N1) virus A/WS/33, influenza (H1N1) virus A/WSN/33, or MLV-GPF pseudoviruses (either H1 or VSV-G envelope proteins).

Viral propagation and titration: influenza A virus A/PR/8/34 H1N1 (ATCC VR-1469), A/WS/33 H1N1 (ATCC VR-1520), A/WSN/33 H1N1 (kind gift of Dr. Peter Palese), A/Udorn/72 H3N2, A/Uruguay/716/2007 H3N2 (CDC#2007731384), A/Brisbane/59/2007 H1N1

(CDC#2008704388), and A/Aichi/2/68 H3N2 (Charles River Labs) were propagated and viral infectivity was titrated as previously described (Huang et al., 2008). Hybrid Moloney/Amphotropic murine leukemia virus (MLV, ATCC VR-1450) was propagated in NIH3T3 cells. WNV (strain 2741) and DNV serotype 2 (New Guinea C strain) viruses were grown on Vero cells (ATCC# CRL-1586) or C6/30 (ATCC# CRL-1660) cells, respectively. Hepatitis C virus JFH1 genotype 2a, and HIV-IIIB were propagated and used as previously described (Brass et al., 2008). HIV-IIIB (HTLV-IIIB/H9) was from the NARRRP and generously donated by Dr. Robert Gallo, Cat. # 398.

West Nile (WNV) and dengue (DNV) virus infections: West Nile (strain 2741) and dengue serotype 2 (New Guinea C strain) viruses were used to infect the IFITM3-silenced HeLa cells at an moi of 0.1 for 24 or 30 h respectively, as reported previously (Krishnan et al., 2008). Infected cells were fixed in 4% PFA and immuno-stained with antibodies detecting viral E-proteins (Chemicon), and imaged by fluorescence microscopy (Zeiss). IFITM3 over-expressing or vector control-A549 or -U20S cells were infected with WNV at an moi of one.

Influenza A virus and MLV infection: Influenza A virus A/PR/8/34 (H1N1) (moi =5), A/Udorn/72 (H3N2) (moi =1), and MLV were used to infect A549 cells expressing different IFITM proteins. 24 hours later, infected cells were labeled with murine anti-influenza viral H1 IgG_{2a} (C179), anti-influenza viral H3 IgG_1 (F49) (Takara Bio. Cat#M145 and M146), or goat anti-MLV env polyclonal antibodies (ATCC), and stained with PE-conjugated anti -mouse or anti-goat secondary antibodies. Cells were then fixed with 1% formaldehyde and analyzed by flow cytometry. For MDCK infections, WSN/33 virus at an moi =0.005 was added to \cell cultures and monitored for cytopathic effect by microscopy. Additional viral infection and IF assays were carried out as described in the respective figure legends.

Flavivirus Viral Like Particle (VLP) and Pseudotyped Virus Production and Infection: MLV-GFP pseudoviruses have been previously described (Huang et al., 2006; Huang et al., 2008). Flavivirus VLP has been described (Hanna et al., 2005), except plasmids encoding structure proteins of WNV (strain NY99), yellow fever virus (strain D17), or Omsk hemorrhagic fever virus (Ref. Seq.: NP_878909.1) were used. VLP and pseudovirus entry in A549 or Vero E6 cells expressing different IFITM proteins was assessed 2 days later by measuring GFP expression by flow cytometry. The level of infection of siRNA-transfected U2OS cells after two days of infection was determined by calculating the percent GPF positive cells by IF using the IXM scanning miscoscope, after fixation with 4% PFA and staining of nuclei with Hoechst 33342.

IF assays: Intracellular HA-staining was performed as above with the exception that after PFA fixation, cells were incubated in 0.1-0.2% Tween 20 (Sigma), then blocked in 1% BSA with 0.3M glycine in D-PBS, prior to staining with the primary antibody. This identical protocol was used with staining for NP (Abcam, AA5H, ab20343, 1:1000), M2 (Abcam, 14C2, ab5416, 1:1000), monoclonal Anti-HA7 from Sigma-Aldrich (Product code H 3663, which recognizes the HA nonapeptide tag on $IFITM3^{R6}$, but not PR8's hemagglutinin (HA)), and the monoclonal antibodies against Human Influenza A virus (H1N1, H2N2), Takara, C179, Cat#M145, (1:1000) which recognizes the HA of WS/33, but not of PR8, and antibody from Takara, F49, Cat#M146, (1:1000), which recognizes the HA of A/Aichi/2/68. HIV replication was detected using the monoclonal antibody, mab-183-H12-5C, generously provided by the NARRRP, Reagent 3537, and kindly contributed by Dr. Bruce Chesebro and Kathy Wehrly. HCV replication was monitored supernatant from anti-HCV core 6G7 hybridoma cells generously provided by Drs. Harry Greenberg and Xiaosong He, Stanford University. Sialic acid staining has been described (Huang et al., 2006; Huang et al., 2008).

siRNAs: The following custom siRNA oligonucleotides (Dharmacon) were used in this study:

NP GGAUCUUAUUUCCUUCGGAGUU (Ge et al., 2003)

HIV-1 Tat CUGCUUGUACCAAUUGCUAUU

All of the following are Dharmacon siRNAs, catalogue numbers are provided, however in the case of the individual duplex oligos these are subject to discontinuation and we therefore strongly suggest careful attention to the catalogue numbers and sequences provided,
All are human-sequence reagents:
Non-targeting control #2 (D-001210-02) UAAGGCUAUGAAGAGAUAC
NFX1 (SMARTpool M-013680-01), PLK1 (M-003290-01)
SART1-1 Dharmacon D-017283-01 Target sequence CCGAAUACCUCACGCCUGA
SART1-2 Dharmacon D-017283-02 Target sequence GCAAGAGCAUGAACGCGAA
SART1-3 Dharmacon D-017283-03 Target sequence GCUACAAACCCGACGUUAA
SART1-4 Dharmacon D-017283-04 Target sequence GAACCGAUCGUGAAUAGGG
COPB1-1 Dharmacon D-017940-01 Target sequence CGACACAGCUAUGUUAGAA
COPB1-2 Dharmacon D-017940-02 Target sequence UAUAAGGUCUGUCAUGCUA
COPB1-3 Dharmacon D-017940-03 Target sequence CCUCAUGACUUCGCAAAUA
COPB1-4 Dharmacon D-017940-04 Target sequence GCUGUUACCGGCCAUAUAA
CALCOCO2 Dharmacon D-010637-01 Target sequence GACAAGAUCUUCCCAGCUA
CALCOCO2 Dharmacon D-010637-03 Target sequence GAAGACAACCCGUGAGUAU
CALCOCO2 Dharmacon D-010637-04 Target sequence CCAAGGAUGAUGAGUAUUA
CALCOCO2 Dharmacon D-010637-17 Target sequence AGACUGAGUGAGAACGAAA
IFITM3-1 Dharmacon D-014116-13 Target sequence ACGUGUUUCUGGUGCUAAA
IFITM3-2 Dharmacon D-014116-14 Target sequence AUGGAUAGAUCAGGAGGCA
IFITM3-3 Dharmacon D-014116-15 Target sequence UGCUGAUCUUCCAGGCCUA
IFITM3-4 Dharmacon D-014116-16 Target sequence UCGUCAUCCCAGUGCUGAU
IFITM3-5 Ambion s195033, Sense GCCUAUGGAUAGAUCAGGATT
IFITM3-6 Ambion s195035, Sense CCCACGUACUCCAACUUCCTT
IFITM3-7 Ambion s237512, Sense UGUCCAAACCUUCUUCUCUTT
Plasmids, and generating stable cell lines: The coding sequence for IFITM3 was obtained from the Vidal Lab Human Orfeome in pDONR-223, after being fully sequence confirmed as correct with the designated Refseq sequence (NM_021034.2), it was recombined into a Gateway-compatible destination vector with a C-terminal HA epitope tag and a Puromycin selectable gene, using LR-clonase (Invitrogen) to produce pMSCV-IFITM3-HA^{6R}. An empty version of the expression vector (pMSCV-puro) was used as control. Human IFITM1, 2 or 3 or mouse Ifitm1, 2 or 3, all without any tags, were cloned into pQCXIP (Clontech) using In Fusion cloning kit (Clontech) to the AgeI and BamHI sites. An empty pQCXIP was used as a control. IFITM protein-transducing pseudovirus was generated as previously described (40). c-myc-taggedIFITM1, 2, or 3 was cloned onto the pQCXIX vector (Clontech), and used to generate transducing virus. For transduction, A549 or VeroE6 cells were incubated with MLV carrying different IFITM genes for 6 hours, and then maintained in regular media. Two days later, cells were challenged with MLV-GFP pseudovirus or VLPs bearing the indicated entry protein. Entry measured by GFP-expression was accessed two days later by flow cytometry. For mixing experiments, U2OS cells were stably transduced with MSCV-P-Discosoma red protein (MSCV-P-DSRed, Clontech) and selected with Puromycin (1.5 ug/ml, Clontech).
Western Analysis, Antibodies: Whole-cell extracts were prepared by cell lysis, equivalent protein content boiled in SDS sample buffer, resolved by SDS/PAGE, transferred to Immobilon–P membrane (Millipore), and probed with the indicated antibodies. Rabbit anti-SART1 was from Bethyl (A301-423A); mouse monoclonal anti-COPB1 (M3A5) was a kind gift from Dr. Victor Hsu (Brigham and Women's Hospital); Purified Rabbit polyclonal to IFITM3 was from Abgent (Cat #AP1153a, along with the corresponding blocking peptide Cat # BP1153); with an additional independent anti-sera from Abcam (#ab74669); Human IFITM1 mouse monoclonal antibody was from Proteintech Group, Inc (Cat# 60074-1); Human IFITM2 rabbit polyclonal antibody was also from Proteintech (Cat# 12769-1); Mouse Ifitm2 rabbit polyclonal was purchased from Santa Cruz Biotechnology (Cat# sc-66828); Anti-fragilis (Ifitm3) rabbit polyclonal antibody was

from Abcam (Cat # ab15592), mouse purified polyclonal to CALCOCO2 was from Abnova (Cat #H00010241-B01p); mouse monoclonal anti-Ran was from BD Biosciences (610340); monoclonal Anti-HA7 from Sigma-Aldrich (Product code H 3663). Murine anti-C9 antibody (1D4) was from Santa Cruz Biotechnology (Cat# sc-57432).

Enrichment Analysis:

Statistical analysis of gene enrichment was performed using a hypergeometric distribution as decribed in the GOhyperGAll module of Bioconductor for gene ontology terms (Gentleman et al., 2004). Briefly, the R program was employed (v2.8.1) with the following command: phyper(x-1, m, n-m, k, lower.tail = FALSE), where x is the number of IDF mapped to a specific terms; m, the total number of genes mapped to that term; n total number of unique genes in the Gene Ontology database; and k, the number of IDFs that are mapped to at least one term in the database. P-values were not corrected for multiple testing. Gene Ontology terms (v1587; May 2009) were obtained from the Gene Ontology web page (Ashburner et al., 2000) and mapping of terms to genes were obtained from the NCBI Gene database (March 17 2009). This analysis was also applied to KEGG Pathways (Kanehisa et al., 2004) Reactome (Vastrik et al., 2007) and protein interactions. Each pathway, reaction, event or the number of interactions for each protein were essentially treated as a Gene Ontology term for the purpose of statistical analysis.

Mapping of genes to the viral lifecycle

Annotations information from these species was used to infer function of human genes. Genes were linked to the lifecycle keywords computationally and for each gene the information was reviewed and the mapping was refined manually. In addition protein interaction were used to map additional genes to genes present in the lifecycle map as long as no conflicting evidence was found for the interaction (e.g. different localization). Protein interactions were obtained from the Human Protein Reference Database (Wheeler et al., 2005), The Biomolecular Interaction Network Database (Bader et al., 2001) and BioGrid (Stark et al., 2006). Protein interactions in human as well as in other species were considered.

SUPPLEMENTAL FIGURE LEGENDS:

Fig. S1. The siRNA screen and enriched candidate molecular function.
A) siRNAs against NXF1 or NP inhibit influenza A infection. (green: HA, blue: nuclei). C, non-targeting control siRNA. 4x.
B) Molecular function analysis for candidate genes found in the siRNA screen for influenza A virus host factors. The significance theshold is indicated by a black line at 1.3 = –log (P = 0.05).

Fig. S2. Protein network extension analysis predicts influenza A virus-dependency factors.
Network showing connections between IDFs identified in the human siRNA screen (blue); the human orthologues of proteins identified in the fly-based screen (pink), factors which were found in both human and fly screens (green). A double border signifies the candidate is present in the Reactome influenza A virus infection pathway (http://www.reactome.org/). To identify potential key intermediates (gray), human and fly host factors detected in the RNAi screens were used to select proteins that are significantly ($p<0.05$) connected given the number of their known interactors (Materials and Methods).

Fig. S3. IFITM3 depletion increases influenza A virus infection.
A) U2OS cells transfected with the indicated siRNAs for 72 h, then infected with influenza A (PR8). At 12 h post-infection, cells were stained for HA (red: HA, blue: nuclei). C = Non-targeting control siRNA, throughout. Numbers indicate percent infection normalized to control /± SD, N=3, throughout. 4x magnification throughout.
B) Primary lung fibroblast cells (WI-38) were transfected with the indicated siRNAs and infected with PR8 72 h later. Twelve h post-infection the cells were stained for HA expression (green: HA, blue: nuclei). Numbers indicate percent infection normalized to control ± SD, n=3.
C) HeLa cells treated as in A, (green: HA, blue: nuclei). Numbers indicate percent infection normalized to control ± SD, n=3.
D) MDCK cells were infected with viral supernatant from the siRNA-transfected HeLa cells in C), after the virus had been activated by incubating with trypsin. Twelve h post-infection the cells were stained for HA expression (red: HA, blue: nuclei). Numbers indicate percent infection normalized to control ± SD, n=3.
E) HeLa-CD4 cells were transfected with the indicated siRNAs for 72 h, then infected with influenza A (WSN/33). At 12 h post-infection, cells were stained for HA (red: HA, blue: nuclei). C = Non-targeting control siRNA, throughout. Numbers indicate percent infection ± SD, n=3.
F) as in E), but siRNA-transfected cells were challenged with HIV-IIIB for 48 h, then stained for the HIV p24 protein as a readout for viral replication (p24: red, nuclei: blue). Numbers indicate percent infection ± SD, n=3.
G) WI-38 cell stained for IFITM3 (left panels, red, primary antibody Abcam ab74669), and glycosylated-proteins using WGA (middle panels, green), and the merged images (right panels, blue: nuclei), 63x.
H) IFITM3 staining is decreased after siRNA-targeting. U20S cells transfected with the indicated siRNAs for 48 h, then left untreated (top panels) or incubated with IFN-γ for 24 h (bottom panels), prior to staining with α-IFITM3 (red, primary antibody Abcam ab74669, nuclei: blue). Non-targeting siRNA, C. 63x.
I) The pattern of IFITM3 staining is similar in U2OS and HeLa cells, and is decreased after siRNA-depletion: Top panels) HeLa cells were treated with the indicated siRNAs for 72 h, then stained with α-IFITM3, (red, primary antibody Abcam ab74669, nuclei: blue). C, non-targeting siRNA, 63x.

Bottom panels) IFITM3 staining with an independently-derived antibody is similar to that already observed and is outcompeted with a blocking peptide. HeLa cells stained for IFITM3 without (left panel) or with (right panel) a blocking peptide, (red, primary antibody Abgent AP1153, nuclei: blue), 63x.

Fig. S4 Depletion of IFITM3 reduces the anti-viral actions of IFN-α. Over-expressed IFITM3 blocks Influenza A Virus Infection.
A) U2OS cells transfected with the indicated siRNAs for 48 h were then incubated in the absence, or presence of IFN-α for 24 h. Cells were subsequently challenged with PR8 for 12 h, then stained for HA expression. C= non-targeting control siRNA. Percent infection ± SD, n =3 throughout.
B) HeLa cells treated as in A. Percent infection ± SD, n=3.
C) A549 or U2OS cells stably over-expressing either IFITM3 or the vector alone (also shown in 4C, D), were infected with influenza A virus H1N1 WSN/33 at the indicated two-fold dilutions of viral supernatant (384 well plates with ~ 60 μl total volume per well). 12 h. later, the cells were fixed and stained for HA expression by IF. Values are representative of 3 independent experiments.
D) MDCK cells stably expressing over-expressing either IFITM3 or the vector alone (also shown in 4G, H), were infected with the indicated viruses for 12 h. then stained for HA expression (green, A/Aichi/2/68, A/WSN/33) or NP expression (green, A/Brisbane/59/07, A/Uruguay/716/07), nuclei:blue. Percent infection ± SD, n=3.
E) 293T cells stably over-expressing IFITM3 or the vector alone were infected with the indicated pseudoparticles for 48 h, or with WSN/33 virus for 12 h. Cells infected with the GFP-expressing pseudoparticles were fixed and imaged at 4x (green: GFP-expression from the integrated MLV proviruses, blue: nuclei). 293T cells infected with WSN/33 were stained for HA expression (red, blue: nuclei). Percent infection ± SD, n=3.
F) 293T cells were assessed by Western blot for the presence of IFITM3 protein.

Fig. S5 IFITM3 is expressed on the cell surface, and does not inhibit HCV infection.
A) Cell surface expression of N-terminally c-myc- tagged IFITM3, measured by flow cytometry using the anti-c-Myc antibody 9E10 and PE-conjugated secondary antibody, is shown for vector and Myc-IFITM3-transduced (IFITM3) A549 cells. Cells were assayed without permeabilization.
B) U2OS cells stably transduced with the empty retroviral vector control or expressing IFITM3-HA^{6R} were fixed, but not permeablized, then stained with the HA7 antibody (HA7) which recognizes the HA-tag on the C-terminus of IFITM3-HA^{6R}, available on the cell surface. Hoechst stained nuclei are also shown (blue). 40x.
C) A549 cells stably over-expressing the indicated IFITM proteins or vector alone, indicated by complementary DNAs (cDNAs) across the top, were assessed for expression by Western blot.
D) Huh 7.5.1 cells stably over-expressing IFITM3 or the vector alone were challenged with the indicated viruses or pseudoparticles for 48 h (HCV JFH1 strain, H5N1-pp), or 12 h (A/WSN/33, A/Aichi/2/68), then stained for HCV core protein (HCV JFH1), HA protein (A/WSN/33, A/Aichi/2/68), or GFP-expression (H5N1-pp), all shown in red, blue: nuclei. Percent infection ± SD, n=3.
E) Huh 7.5.1 cells stably over-expressing IFITM3 or vector alone were assessed for expression by Western blot.

Fig. S6 Human and mouse IFITM1, 2, 3 protein alignment. The two transmembrane domains as predicted by UnitprotKB, are shown in bold and underlined. The alignment was performed with ClustalIW. Red: hydrophobic/aromatic amino acids (aa), Blue: acidic aa, Magenta: basic aa, Green: hydroxyl, amine aa. * identical aa, : conservative aa substitution, . semi-conservative substitution.

Fig. S7 Extended Species IFITM1, 2, 3 and 5 protein alignment. The alignment was performed with ClustalIW. Red: hydrophobic/aromatic amino acids (aa), Blue: acidic aa, Magenta: basic aa, Green: hydroxyl, amine aa. * identical aa, : conservative aa substitution, . semi-conservative substitution.

A

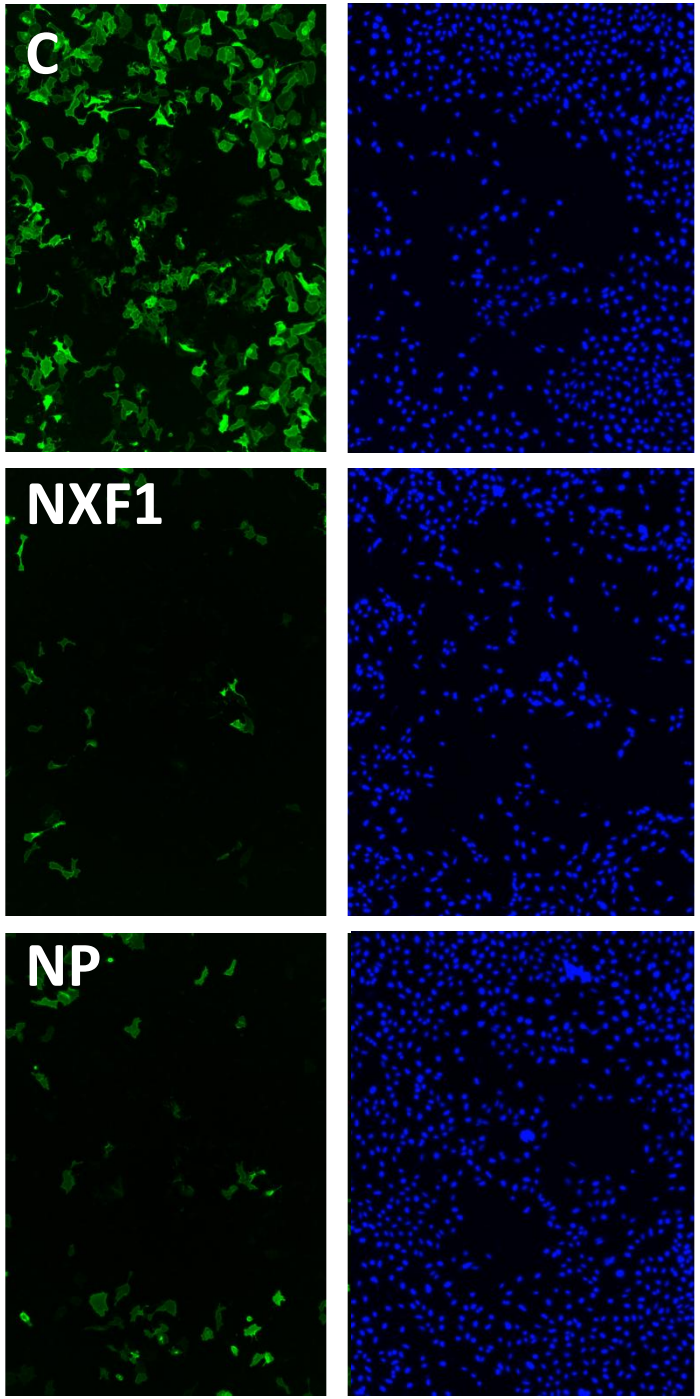
C
NXF1
NP

B

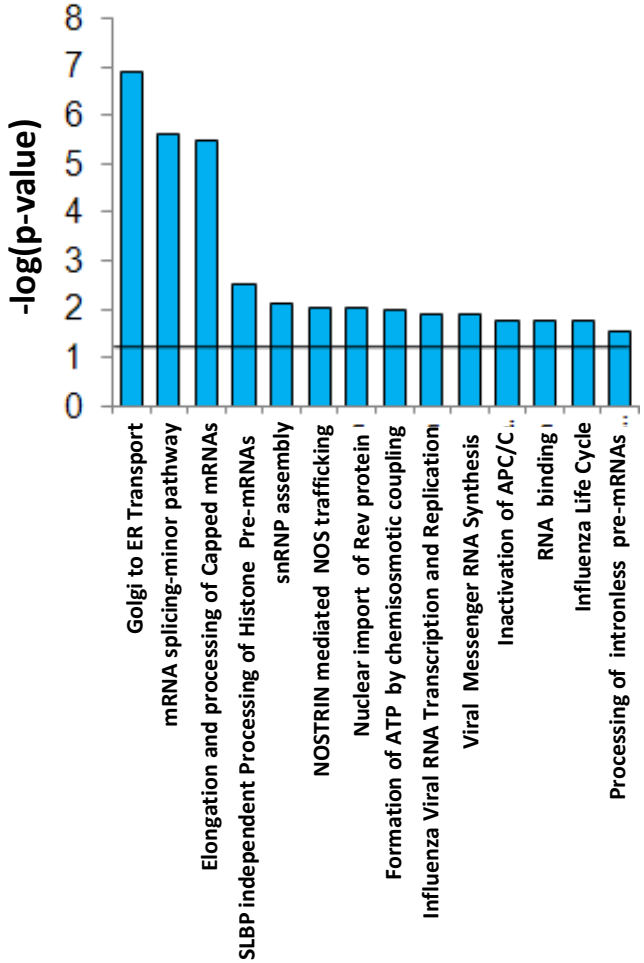
-log(p-value)
8
7
6
5
4
3
2
1
0
Golgi to ER Transport
mRNA splicing-minor pathway
Elongation and processing of Capped mRNAs
SLBP independent Processing of Histone Pre-mRNAs
snRNP assembly
NOSTRIN mediated NOS trafficking
Nuclear import of Rev protein
Formation of ATP by chemisosmotic coupling
Influenza Viral RNA Transcription and Replication
Viral Messenger RNA Synthesis
Inactivation of APC/C
RNA binding
Influenza Life Cycle
Processing of intronless pre-mRNAs

Fig. S1

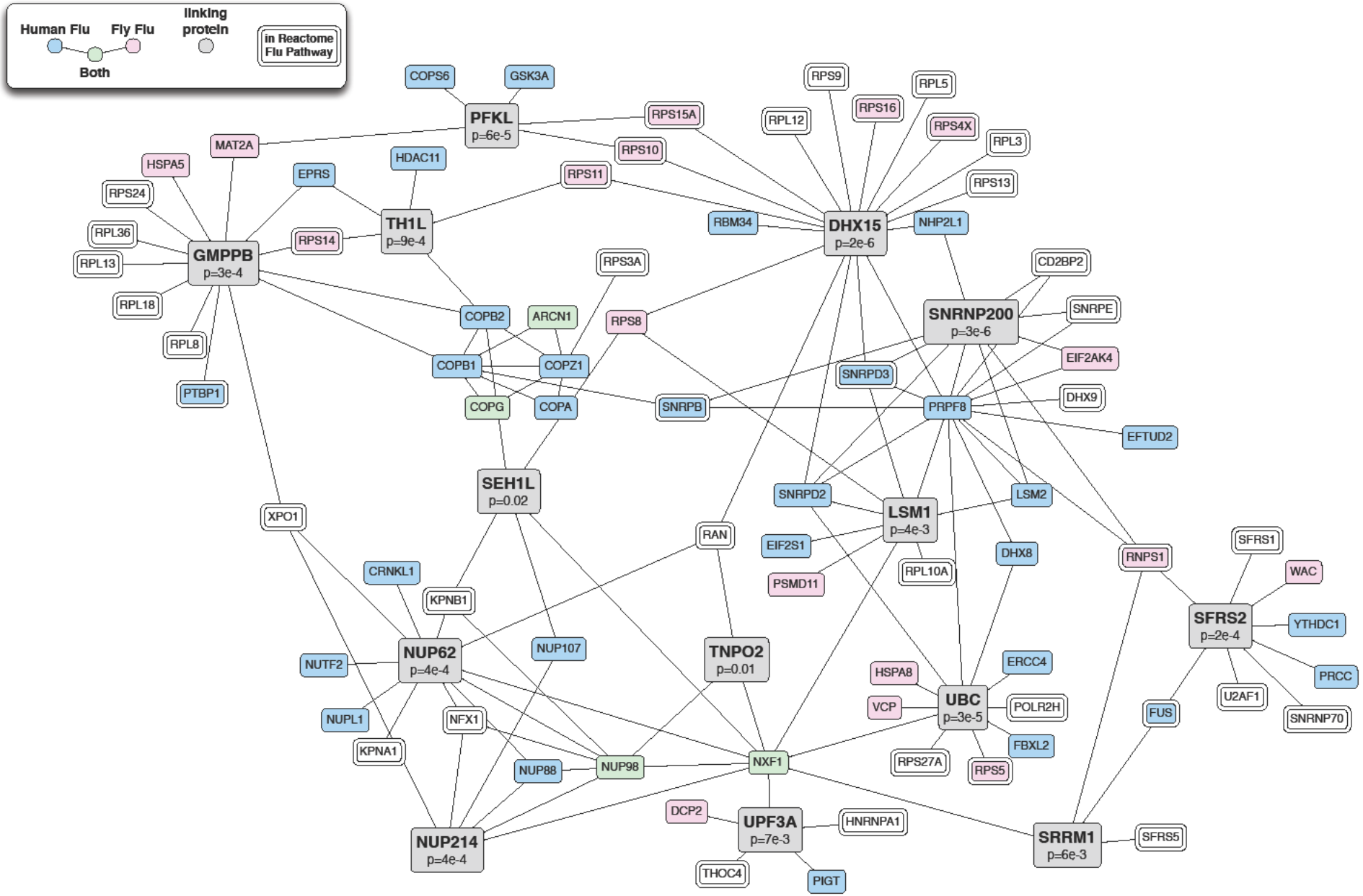
Human Flu
Fly Flu
Both
linking protein
in Reactome Flu Pathway
COPS6
GSK3A
PFKL
p=6e-5
MAT2A
HDAC11
HSPA5
EPRS
RPS24
TH1L
p=9e-4
RPL36
RPS14
RPL13
GMPPB
p=3e-4
RPL18
RPL8
PTBP1
RPS15A
RPS10
RPS11
RPS3A
RPS8
COPB2
ARCN1
COPB1
COPZ1
COPG
COPA
SEH1L
p=0.02
XPO1
CRNKL1
KPNB1
NUTF2
NUP62
p=4e-4
NUP107
NUPL1
NFX1
KPNA1
NUP88
NUP98
NUP214
p=4e-4
RAN
TNPO2
p=0.01
DCP2
UPF3A
p=7e-3
HNRNPA1
THOC4
PIGT
NXF1
RPS9
RPL5
RPS16
RPL12
RPS4X
RPL3
RPS13
RBM34
DHX15
p=2e-6
NHP2L1
CD2BP2
SNRNP200
p=3e-6
SNRPE
EIF2AK4
SNRPD3
DHX9
SNRPB
PRPF8
EFTUD2
SNRPD2
LSM1
p=4e-3
LSM2
EIF2S1
PSMD11
RPL10A
DHX8
HSPA8
VCP
UBC
p=3e-5
ERCC4
POLR2H
FBXL2
RPS27A
RPS5
RNPS1
SFRS1
WAC
SFRS2
p=2e-4
YTHDC1
PRCC
U2AF1
SNRNP70
FUS
SRRM1
p=6e-3
SFRS5

Fig. S2

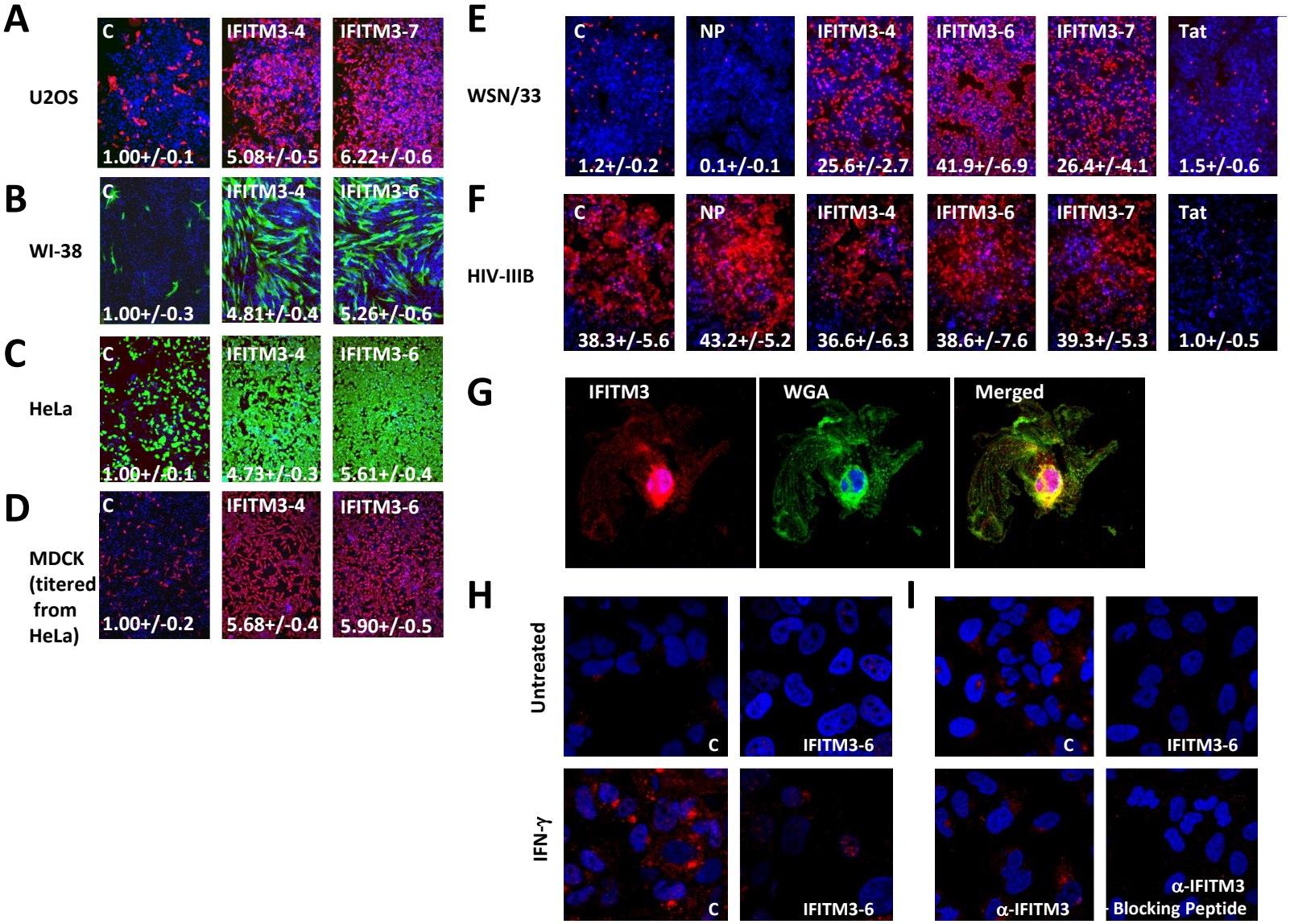
A
U2OS
C
1.00+/-0.1
IFITM3-4
5.08+/-0.5
IFITM3-7
6.22+/-0.6
B
WI-38
C
1.00+/-0.3
IFITM3-4
4.81+/-0.4
IFITM3-6
5.26+/-0.6
C
HeLa
C
1.00+/-0.1
IFITM3-4
4.73+/-0.3
IFITM3-6
5.61+/-0.4
D
MDCK (titered from HeLa)
C
1.00+/-0.2
IFITM3-4
5.68+/-0.4
IFITM3-6
5.90+/-0.5
E
WSN/33
C
1.2+/-0.2
NP
0.1+/-0.1
IFITM3-4
25.6+/-2.7
IFITM3-6
41.9+/-6.9
IFITM3-7
26.4+/-4.1
Tat
1.5+/-0.6
F
HIV-IIIB
C
38.3+/-5.6
NP
43.2+/-5.2
IFITM3-4
36.6+/-6.3
IFITM3-6
38.6+/-7.6
IFITM3-7
39.3+/-5.3
Tat
1.0+/-0.5
G
IFITM3
WGA
Merged
H
Untreated
IFN-γ
C
IFITM3-6
C
IFITM3-6
I
C
IFITM3-6
α-IFITM3
α-IFITM3 Blocking Peptide

Fig. S3

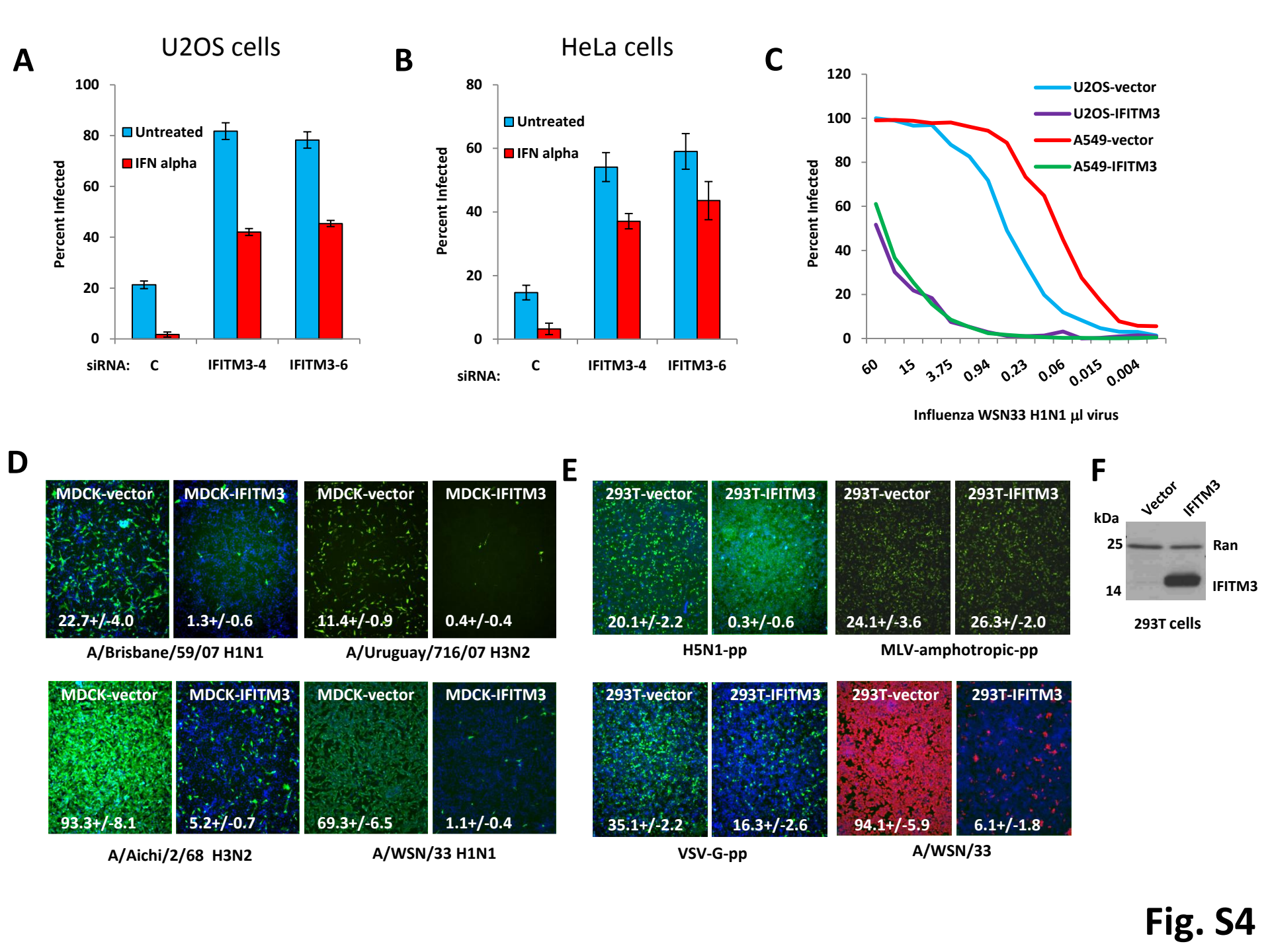
A
U2OS cells
Percent Infected
Untreated
IFN alpha
siRNA: C IFITM3-4 IFITM3-6
B
HeLa cells
Percent Infected
Untreated
IFN alpha
siRNA: C IFITM3-4 IFITM3-6
C
Percent Infected
U2OS-vector
U2OS-IFITM3
A549-vector
A549-IFITM3
60 15 3.75 0.94 0.23 0.06 0.015 0.004
Influenza WSN33 H1N1 µl virus
D
MDCK-vector
MDCK-IFITM3
22.7+/-4.0
1.3+/-0.6
11.4+/-0.9
0.4+/-0.4
A/Brisbane/59/07 H1N1
A/Uruguay/716/07 H3N2
93.3+/-8.1
5.2+/-0.7
69.3+/-6.5
1.1+/-0.4
A/Aichi/2/68 H3N2
A/WSN/33 H1N1
E
293T-vector
293T-IFITM3
20.1+/-2.2
0.3+/-0.6
24.1+/-3.6
26.3+/-2.0
H5N1-pp
MLV-amphotropic-pp
35.1+/-2.2
16.3+/-2.6
94.1+/-5.9
6.1+/-1.8
VSV-G-pp
A/WSN/33
F
Vector
IFITM3
kDa
25
14
Ran
IFITM3
293T cells

Fig. S4

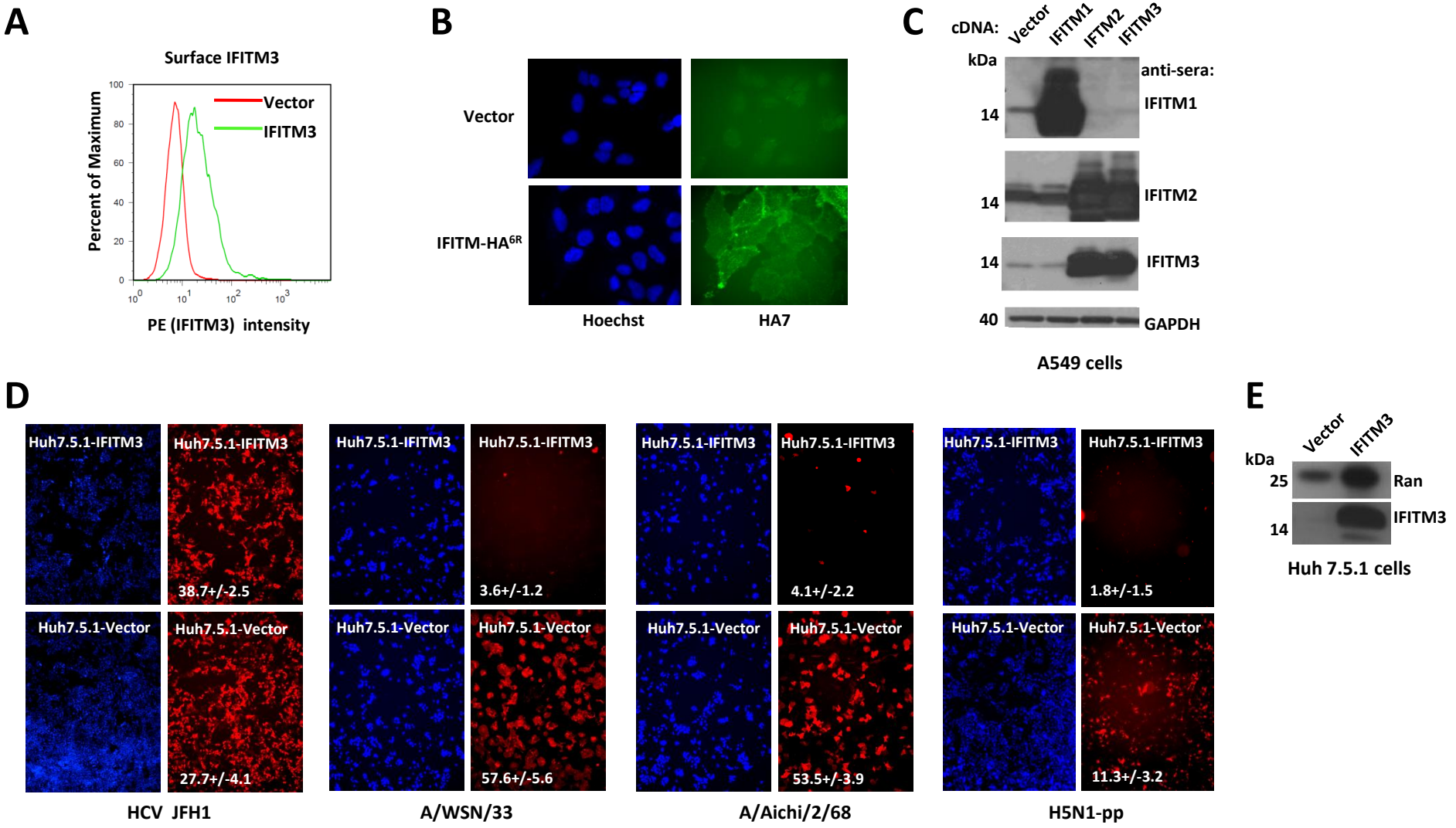
A
Surface IFITM3
Percent of Maximum
Vector
IFITM3
PE (IFITM3) intensity
B
Vector
IFITM-HA6R
Hoechst
HA7
C
cDNA:
Vector
IFITM1
IFTM2
IFITM3
kDa
anti-sera:
14
IFITM1
14
IFITM2
14
IFITM3
40
GAPDH
A549 cells
D
Huh7.5.1-IFITM3
Huh7.5.1-Vector
38.7+/-2.5
27.7+/-4.1
3.6+/-1.2
57.6+/-5.6
4.1+/-2.2
53.5+/-3.9
1.8+/-1.5
11.3+/-3.2
HCV JFH1
A/WSN/33
A/Aichi/2/68
H5N1-pp
E
Vector
IFITM3
kDa
25
Ran
14
IFITM3
Huh 7.5.1 cells

Fig. S5

A


Mouse_Ifitm3 MNHTSQAFITAASGGQPPNYERIKEEYEVAEMGAPHGSASVRTTVINMPREVSVPDHVVW 60
Mouse_Ifitm2 MSHNSQAFLSTNAG-LPPSYETIKEEYGVTELGEPSNSAVVRTTVINMPREVSVPDHVVW 59
Mouse_Ifitm1 ----------MPKEQQEVVVLGSPHISTSATATTINMP-EISTPDHVVW 38
Human_IFITM3 MNHTVQTFFSPVNSGQPPNYEMLKEEHEVAVLGAPHNPAPPTSTVIHIRSETSVPDHVVW 60
Human_IFITM2 MNHIVQT-FSPVNSGQPPNYEMLKEEQEVAMLGGPHNPAPPTSTVIHIRSETSVPDHVVW 59
Human_IFITM1 ----------MHKEEHEVAVLGPPPSTILPRSTVINIHSETSVPDHVVW 39
Mouse_Ifitm3 SLFNTLFMNFCCLGFIAYAYSVKSRDRKMVGDVTGAQAYASTAKCLNISTLVLSILMVVI 120
Mouse_Ifitm2 SLFNTLFFNACCLGFVAYAYSVKSRDRKMVGDVVGAQAYASTAKCLNISSLIFSILMVII 119
Mouse_Ifitm1 SLFNTLFMNFCCLGFVAYAYSVKSRDRKMVGDTTGAQAFASTAKCLNISSLFFTILTAIV 98
Human_IFITM3 SLFNTLFMNPCCLGFIAFAYSVKSRDRKMVGDVTGAQAYASTAKCLNIWALILGILMTIL 120
Human_IFITM2 SLFNTLFMNTCCLGFIAFAYSVKSRDRKMVGDVTGAQAYASTAKCLNIWALILGIFMTIL 119
Human_IFITM1 SLFNTLFLNWCCLGFIAFAYSVKSRDRKMVGDVTGAQAYASTAKCLNIWALILGILMTIG 99
Mouse_Ifitm3 TIV-----SVIIIVLNAQN-LHT--- 137
Mouse_Ifitm2 CIIIFSTTSVVVFQSFAQRTPHSGF- 144
Mouse_Ifitm1 VIV------VCAIR---------- 106
Human_IFITM3 LIVIPVL----------IFQAYG-- 133
Human_IFITM2 LVIIPVL----------VVQAQR-- 132
Human_IFITM1 FILLLVFGSVTVYHIMLQIIQEKRGY 125

Fig. S6

```
Rainbow_Trout_IFITM3|NP_001118      --------MDQPPPYQPEFVPMKGNKYMRLEDTHGAPKFQHTVVLGQPQP 42
Rainbow_Trout_IFITM2|CAC85160.      --------MDQSPSYQPEFVPMNGNKYMRLEDPHGAPKFQHTVVLGLPQP 42
Xenopus_IFITM1|NP_001123403.1       --------MKSSGSLQP---PAYDNQQETREFMVLPSQPQSTVVN--IQP 37
Mouse_IFITM2|NP_109619.1            MSHNSQAFLSTNAG-LPPSYETIKEEY-GVTELGEPSNSAVVRTTVINMP 48
Mouse_IFITM3|NP_079654.1            MNHTSQAFITAASGGQPPNYERIKEEY-EVAEMGAPHGSASVRTTVINMP 49
Mouse_IFITM1|NP_081096.3            ----------------------MPKEQQ-EVVVLGSPHISTSATATTINMP 28
Chimp_IFITM1|XP_001144684.1         ----------------------MHKEEH-EVAVLGAPPSTILPRSTVINIH 28
Chimp_IFITM2|XP_508190.1            MNHIVQT-FSPVNSGQPPNYEMLKEEQ-EVAMLGAPHNPAPPMSTVIHIR 48
Chimp_IFITM3|XP_001145216.1         MNHTVQTFFSPVNSGQPPNYEMLKEEH-EVAVLGAPHNPAPPMSTVIHIR 49
Pig_IFITM1|ABX75538.1               ----------------------MIKSQH-EMDGLGAPQTSAPVATTVITIP 28
Red_Jungle_Fowl|XP_IFITM142092      ----------------------MQSYP-QHTSINMP-SYGQDVTTTIPIS 26
Red_Jungle_Fowl_IFITM5|XP_4209      ----------------------MDTSYPREDYLPMTSHKRDSSPTTATSA-- 28
Mouse_IFITM5|ref|NP_444318.1        ----------------------MDTSYPREDPRAPSSRKADAAAHTALSMGT 30
Electric_Ray_IFITM|Q91499.1         ----------------------MEY-RTDQVPMSPRSVQGAPGTLPIR-- 25

Rainbow_Trout_IFITM3|NP_001118      VVPHPRDHIIWSLCSLVYCNPFCLGMLAVYFSIKSRDRKMVGDLEGARKH 92
Rainbow_Trout_IFITM2|CAC85160.      VVPQPRDHIIWSLCSLVYGNPLCLGMLAVYFSIKSRDRKMVGDLEGARKH 92
Xenopus_IFITM1|NP_001123403.1       SEEPQKDHLVWSIFNLVYCNFCCLGLLALLFSVKSRDRKQFRDTSGAKHY 87
Mouse_IFITM2|NP_109619.1            REVSVPDHVVWSLFNTLFFNACCLGFVAYAYSVKSRDRKMVGDVVGAQAY 98
Mouse_IFITM3|NP_079654.1            REVSVPDHVVWSLFNTLFMNFCCLGFIAYAYSVKSRDRKMVGDVTGAQAY 99
Mouse_IFITM1|NP_081096.3            -EISTPDHVVWSLFNTLFMNFCCLGFVAYAYSVKSRDRKMVGDTTGAQAF 77
Chimp_IFITM1|XP_001144684.1         SETSVPDHVVWSLFNTLFLNWCCLGFIAFAYSVKSRDRKMVGDVTGAQAY 78
Chimp_IFITM2|XP_508190.1            SETSVPDHVVWSLFNTLFMNPCCLGFIAFAYSVKSRDRKMVGDVTGAQAY 98
Chimp_IFITM3|XP_001145216.1         SETSVPDHVVWSLFNTLFMNPCCLGFIAFAYSVKSRDRKMVGDVTGAQAY 99
Pig_IFITM1|ABX75538.1               RETSVPDHIVWSLFNTLFLNWCCLGFVAFAYSVKARDRKMVGDIIGAQSY 78
Red_Jungle_Fowl|XP_IFITM142092      PQPPPKDFVLWSLFNFVLCNAFCLGLCALSYSIKSRDRIIAKDFVGASSY 76
Red_Jungle_Fowl_IFITM5|XP_4209      P---PRDHLIWSIFNTIYMNFCCLGFVALAFSVKARDRKVAGDVEAARRF 75
Mouse_IFITM5|ref|NP_444318.1        PGPTPRDHMLWSVFSTMYLNLCCLGFLALVHSVKARDQKMAGNLEAARQY 80
Electric_Ray_IFITM|Q91499.1         ------DHLPWSIFNLFYMNVCCLGLTAMIFSVKSRDRKVVGDVEGARHY 69
                                          *.: **: . .  *  ***: *  .*:*:**:    :  .*  .

Rainbow_Trout_IFITM3|NP_001118      GKTACCFNTVTLTLAILGLLFFFITYGIIIYQVAH--------------- 127
Rainbow_Trout_IFITM2|CAC85160.      GKTARCFNVVTLTLVILGLLFLFIIYGFFIYNISHL------------- 128
Xenopus_IFITM1|NP_001123403.1       ATTSRSLNIATTVLSILCFLIFIILYFVGIFAIRH--------------- 122
Mouse_IFITM2|NP_109619.1            ASTAKCLNISSLIFSILMVIICIIIFSTTSVVVFQSFAQRTPHSGF---- 144
Mouse_IFITM3|NP_079654.1            ASTAKCLNISTLVLSILMVVITIV-----SVIIIVLNAQN-LHT------ 137
Mouse_IFITM1|NP_081096.3            ASTAKCLNISSLFFTILTAIVVIV------VCAIR--------------- 106
Chimp_IFITM1|XP_001144684.1         ASTAKCLNIWALILGILMTIGFILLLVFGSVTVYHIMLQIIQEKRGY--- 125
Chimp_IFITM2|XP_508190.1            ASTAKCLNIWALILGILMTIGFILLLVFGSVTVYHIMLQIIQEKRGY--- 145
Chimp_IFITM3|XP_001145216.1         ASTAKCLNIWALILGILMTILLIVIPVL------------IFQAYG---- 133
Pig_IFITM1|ABX75538.1               ASTAKCLNIWALILGLILTIGATVLLVFVYITAYH-MLERAKSNRGY--- 124
Red_Jungle_Fowl|XP_IFITM142092      GRTAKIFNIFAFCVGLLVTILSIVLVFLYLPLYTVRP------------- 113
Red_Jungle_Fowl_IFITM5|XP_4209      SSKARCYNALATAGSVLLPILLAALVVTGVLHLSKLAQDSVGFFSSQFSA 125
Mouse_IFITM5|ref|NP_444318.1        GSKAKCYNILAAMWTLVPPLLLLGLVVTGALHLSKLAKDSAAFFSTKFDE 130
Electric_Ray_IFITM|Q91499.1         GSTARSLNIAATVLGILLIIILIGLAATGTIQALKYKG------------ 107
                                    . .:   *  :    ::  :

Rainbow_Trout_IFITM3|NP_001118      ------
Rainbow_Trout_IFITM2|CAC85160.      ------
Xenopus_IFITM1|NP_001123403.1       ------
Mouse_IFITM2|NP_109619.1            ------
Mouse_IFITM3|NP_079654.1            ------
Mouse_IFITM1|NP_081096.3            ------
Chimp_IFITM1|XP_001144684.1         ------
Chimp_IFITM2|XP_508190.1            ------
Chimp_IFITM3|XP_001145216.1         ------
Pig_IFITM1|ABX75538.1               ------
Red_Jungle_Fowl|XP_IFITM142092      ------
Red_Jungle_Fowl_IFITM5|XP_4209      SDDEDK 131
Mouse_IFITM5|ref|NP_444318.1        EDYN-- 134
Electric_Ray_IFITM|Q91499.1         ------
```

Fig. S7

SUPPLEMENTAL REFERENCES:

Ashburner, M., Ball, C.A., Blake, J.A., Botstein, D., Butler, H., Cherry, J.M., Davis, A.P., Dolinski, K., Dwight, S.S., Eppig, J.T., *et al.* (2000). Gene ontology: tool for the unification of biology. The Gene Ontology Consortium. Nat Genet *25*, 25-29.

Bader, G.D., Donaldson, I., Wolting, C., Ouellette, B.F., Pawson, T., and Hogue, C.W. (2001). BIND--The Biomolecular Interaction Network Database. Nucleic Acids Res *29*, 242-245.

Brass, A.L., Dykxhoorn, D.M., Benita, Y., Yan, N., Engelman, A., Xavier, R.J., Lieberman, J., and Elledge, S.J. (2008). Identification of host proteins required for HIV infection through a functional genomic screen. Science *319*, 921-926.

Ge, Q., McManus, M.T., Nguyen, T., Shen, C.H., Sharp, P.A., Eisen, H.N., and Chen, J. (2003). RNA interference of influenza virus production by directly targeting mRNA for degradation and indirectly inhibiting all viral RNA transcription. Proc Natl Acad Sci U S A *100*, 2718-2723.

Gentleman, R.C., Carey, V.J., Bates, D.M., Bolstad, B., Dettling, M., Dudoit, S., Ellis, B., Gautier, L., Ge, Y., Gentry, J., *et al.* (2004). Bioconductor: open software development for computational biology and bioinformatics. Genome Biol *5*, R80.

Hao, L., Sakurai, A., Watanabe, T., Sorensen, E., Nidom, C.A., Newton, M.A., Ahlquist, P., and Kawaoka, Y. (2008). Drosophila RNAi screen identifies host genes important for influenza virus replication. Nature *454*, 890-893.

Hausmann, S., Zheng, S., Costanzo, M., Brost, R.L., Garcin, D., Boone, C., Shuman, S., and Schwer, B. (2008). Genetic and biochemical analysis of yeast and human cap trimethylguanosine synthase: functional overlap of 2,2,7-trimethylguanosine caps, small nuclear ribonucleoprotein components, pre-mRNA splicing factors, and RNA decay pathways. J Biol Chem *283*, 31706-31718.

Huang, I.C., Bosch, B.J., Li, F., Li, W., Lee, K.H., Ghiran, S., Vasilieva, N., Dermody, T.S., Harrison, S.C., Dormitzer, P.R., *et al.* (2006). SARS coronavirus, but not human coronavirus NL63, utilizes cathepsin L to infect ACE2-expressing cells. J Biol Chem *281*, 3198-3203.

Huang, I.C., Li, W., Sui, J., Marasco, W., Choe, H., and Farzan, M. (2008). Influenza A virus neuraminidase limits viral superinfection. J Virol *82*, 4834-4843.

Kanehisa, M., Goto, S., Kawashima, S., Okuno, Y., and Hattori, M. (2004). The KEGG resource for deciphering the genome. Nucleic Acids Res *32*, D277-280.

Krishnan, M.N., Ng, A., Sukumaran, B., Gilfoy, F.D., Uchil, P.D., Sultana, H., Brass, A.L., Adametz, R., Tsui, M., Qian, F., *et al.* (2008). RNA interference screen for human genes associated with West Nile virus infection. Nature *455*, 242-245.

Lamb, R.A., and Krug, R.M. (2001). Orthomyxoviridae: The viruses and their replication., 4th edn (Philadelphia, Lippincott Williams and Wilkins).

Lange, U.C., Adams, D.J., Lee, C., Barton, S., Schneider, R., Bradley, A., and Surani, M.A. (2008). Normal germ line establishment in mice carrying a deletion of the Ifitm/Fragilis gene family cluster. Mol Cell Biol *28*, 4688-4696.

Lemm, I., Girard, C., Kuhn, A.N., Watkins, N.J., Schneider, M., Bordonne, R., and Luhrmann, R. (2006). Ongoing U snRNP biogenesis is required for the integrity of Cajal bodies. Mol Biol Cell *17*, 3221-3231.

Mouaikel, J., Verheggen, C., Bertrand, E., Tazi, J., and Bordonne, R. (2002). Hypermethylation of the cap structure of both yeast snRNAs and snoRNAs requires a conserved methyltransferase that is localized to the nucleolus. Mol Cell *9*, 891-901.

Stark, C., Breitkreutz, B.J., Reguly, T., Boucher, L., Breitkreutz, A., and Tyers, M. (2006). BioGRID: a general repository for interaction datasets. Nucleic Acids Res *34*, D535-539.
Vastrik, I., D'Eustachio, P., Schmidt, E., Gopinath, G., Croft, D., de Bono, B., Gillespie, M., Jassal, B., Lewis, S., Matthews, L., *et al.* (2007). Reactome: a knowledge base of biologic pathways and processes. Genome Biol *8*, R39.

Wheeler, D.L., Barrett, T., Benson, D.A., Bryant, S.H., Canese, K., Church, D.M., DiCuccio, M., Edgar, R., Federhen, S., Helmberg, W., *et al.* (2005). Database resources of the National Center for Biotechnology Information. Nucleic Acids Res *33*, D39-45.